The Journal of Immunology

Cytokine-Induced Hepatic Apoptosis Is Dependent on FGL2/Fibroleukin: The Role of Sp1/Sp3 and STAT1/PU.1 Composite *cis* Elements

Mingfeng Liu, Michael Mendicino, Qin Ning, Anand Ghanekar, Wei He, Ian McGilvray, Itay Shalev, David Pivato, David A. Clark, M. James Phillips and Gary A. Levy

J Immunol 2006; 176:7028-7038; ;
doi: 10.4049/jimmunol.176.11.7028
http://www.jimmunol.org/content/176/11/7028

The Journal of Immunology is published twice each month by
The American Association of Immunologists, Inc.,
1451 Rockville Pike, Suite 650, Rockville, MD 20852

Print ISSN: 0022-1767 Online ISSN: 1550-6606.

Cytokine-Induced Hepatic Apoptosis Is Dependent on FGL2/Fibroleukin: The Role of Sp1/Sp3 and STAT1/PU.1 Composite *cis* Elements

Mingfeng Liu,* Michael Mendicino,* Qin Ning,† Anand Ghanekar,* Wei He,* Ian McGilvray,* Itay Shalev,* David Pivato,* David A. Clark,* M. James Phillips,* and Gary A. Levy[1]*

Previous studies from our laboratory have shown that fulminant hepatitis caused by the mouse hepatitis virus, MHV-3, is dependent on production of the novel immune coagulant fgl2/fibroleukin. In this study, we investigate the role of IFN-γ and TNF-α in the induction of fgl2 expression and fgl2-dependent hepatic apoptosis. Infusion of IFN-γ in combination with TNF-α through the portal vein of *fgl2*$^{+/+}$ mice led to widespread hepatic apoptosis and fibrin deposition. Livers from *fgl2*$^{-/-}$ mice were normal, although strong expression of the fgl2 knockout reporter gene *Lac Z* was seen in both resident hepatic macrophages and endothelial cells. In vitro, IFN-γ and TNF-α induced fgl2 expression in a macrophage and endothelial cell-specific manner. In macrophages (peritoneal and RAW 264.7 cells), IFN-γ, but not IFN-α, LPS, TNF-α, or IL-1 induced fgl2 mRNA transcription and protein expression, while in endothelial cells TNF-α, but not IFN-γ, induced fgl2 transcription. In addition, while TNF-α enhanced IFN-γ-induced macrophage fgl2 transcription, IFN-γ also enhanced TNF-α-induced endothelial cell fgl2 transcription. The induction of fgl2 by IFN-γ in macrophages involved a STAT1-dependent pathway, involving the composite *cis* elements Sp1/Sp3 and GAS/PU.1. The latter interacted with IFN-γ-dependent Sp1/Sp3, STAT1, and the Ets family of transcription factors member PU.1. The interaction of PU.1 with the IFN-γ-activated sequence/Ets family of transcription factors site determined the macrophage-specific induction of fgl2 by IFN-γ. Overall, this study demonstrates that IFN-γ and TNF-α induce hepatocyte apoptosis in vivo, which is dependent on induction of fgl2, and defines the molecular basis of transcription of fgl2 in vitro. *The Journal of Immunology,* **2006, 176: 7028–7038.**

Cytokines play an important role in the pathogenesis of both experimental and human acute and chronic liver diseases including viral hepatitis B (HBV),[2] hepatitis C, experimental hepatitis in mice induced by mouse hepatitis virus 3 (MHV-3), autoimmune hepatitis, alcohol-induced hepatitis, and hepatitis produced by hepatotoxins including Con A (1–3). Although we have reported a critical role for the procoagulant molecule fgl2 in MHV-3-induced fulminant hepatitis, its role in cytokine-dependent liver damage in general is unclear.

Recently, it has been reported that Con A-induced hepatitis is an IFN-γ-dependent event mediated by the STAT1. IFN-γ has also been implicated in both LPS- and D-galactosamine-induced liver injury in animals and in chronic hepatitis C infection in humans (3, 4). By transgenic approaches, it has been shown that overexpression of IFN-γ in the liver directly can produce chronic active hepatitis (5) and IFN-γ is critical to the pathogenesis of acute hepatitis in an HBV transgenic model system (6).

There is considerable information concerning the mechanisms by which IFN-γ activates gene expression. Following IFN-γ binding, the IFN-γR oligomerizes and brings the JAKs into juxtaposition, leading to their cross-phosphorylation and activation (7, 8). The STATs, which are recruited to the JAK-receptor complex via their Src homology 2 domain, are phosphorylated on a conserved tyrosine residue. This phosphorylation results in STAT dimerization to form a protein complex denoted as γ-activated factor which relocates to the nucleus and regulates expression of multiple target genes through the IFN-γ-activated sequence (GAS), such as ICAM-1 (9–11). Recent studies have also shown that a JAK-activated, STAT1-independent pathway exists for IFN-γ-regulated genes (7). This STAT1-independent pathway is as equally important as the STAT1-dependent pathway in contribution to antiviral responses, and to the control of proliferation and tumor suppression (7). For example, IFN-γ can regulate gene expression through a JAK1-dependent, STAT1-independent pathway (7). In addition, IFN-γ can induce C/EBP-β transcription and regulates the transcription of IFN-γ-regulated factor 9 (IRF-9) through novel IFN-γ-activated transcriptional elements) that are different from GAS (12). In addition, an E box, distinct from GAS, and possible cooperative *cis* elements, have been found to be totally responsible for IFN-γ induction of the fourth component of human complement (C4) (13). These findings indicate that IFN-γ may act via a variety of intracellular pathways to regulate gene expression relevant to induction of hepatic inflammation.

In MHV-3-induced liver injury, intravascular fibrin deposition and subsequent liver cell (hepatocyte) apoptosis are a consequence of MHV-3 induction of the immune coagulant fgl2/fibroleukin in macrophages and endothelial cells (14, 15). Infusion of mAbs against fgl2 prevents MHV-3-induced liver injury and subsequent

*Multi-Organ Transplant Program, Toronto General Hospital, University of Toronto, Toronto, Ontario, Canada; and †Department of Infectious Disease, Tongji Hospital, Medical College, Wuhan, China

Received for publication October 6, 2005. Accepted for publication March 13, 2006.

The costs of publication of this article were defrayed in part by the payment of page charges. This article must therefore be hereby marked *advertisement* in accordance with 18 U.S.C. Section 1734 solely to indicate this fact.

[1] Address correspondence and reprint requests to Dr. Gary A. Levy, Multi-Organ Transplant Program, Toronto General Hospital, University of Toronto, 585 University Avenue, NCSB11-1236, Toronto, ON M5G 2N2 Canada. E-mail address: glfgl2@attglobal.net

[2] Abbreviations used in this paper: HBV, viral hepatitis B; MHV-3, mouse hepatitis virus 3; GAS, IFN-γ-activated sequence; IRF, IFN-γ-regulated factor; β-gal, β-galactosidase; siRNA, small-interfering RNA; ChiP, chromatin immunoprecipitation assay; IP, immunoprecipitated; Pol II, polymerase II.

0022-1767/06/$02.00

mortality, supporting a pivotal role for fgl2 in the pathogenesis of MHV-3-induced liver damage (16). Furthermore, mice in which fgl2 was deleted by targeted recombination ($fgl2^{-/-}$) had a marked reduction in MHV-3-induced liver injury (17). Although the nucleocapsid (core) protein of MHV-3 was shown to induce fgl2 expression, there are other factors that are thought to contribute to the regulation of fgl2 transcription (14, 15). It has been reported that induction of IFN-γ and TNF-α by macrophages is a critical determinant of both the liver cell death and subsequent morbidity/mortality associated with MHV-3 infection (18). Furthermore, IFN-γ has also previously been reported to induce fgl2 transcription in BALB/cJ peritoneal macrophages in vitro (19).

In this report, we demonstrate that IFN-γ in combination with TNF-α induces hepatocyte apoptosis in vivo which is fgl2 dependent. We further demonstrate that the STAT1-related signaling pathway and Sp1/Sp3-STAT1/PU.1 transcriptional complex are involved in the regulation of fgl2 transcription in vitro.

Materials and Methods

Cells and cytokines

Peritoneal macrophages were harvested from BALB/cJ mice 5 days after i.p. administration of 1.5 ml of 5% thioglycolate (Difco Laboratories) as described previously (20). The murine macrophage cell line, RAW 267.4 (RAW), which was derived from BALB/cJ mice, was obtained from the American Type Culture Collection (ATCC). Cells were maintained in DMEM supplemented so as to contain 10% FBS and maintained as instructed according to ATCC protocols. Cytokines IL-1, IL-6, IFN-γ, TNF-α, and IFN-α were purchased from BD Pharmingen. LPS was purchased from Sigma-Aldrich.

Mice

Production of mice deficient in fgl2 has been described previously (17). Mice of the $fgl2^{-/-}$ genotype backcrossed onto C57BL/6 for 10 generations were used for the series of experiments described below. The LacZ reporter and *PGK-neo* gene were inserted within the first of two coding exons of the *fgl2* gene enabled detection of fgl2 transcription by β-galactosidase (β-gal) expression.

Histology

Livers were removed from all euthanized animals and analyzed for histology. For histological examination and quantification of hepatic necrosis and apoptosis, liver tissue was fixed in 10% buffered formalin for 4 h followed by routine tissue processing and staining using an automated tissue processor, following which the tissue blocks were embedded in paraffin. Livers were then sectioned 5-μm thick and stained with H&E and with martius/scarlet/blue. Tissue sections of liver were also stained for assessment of apoptosis using a standard laboratory TUNEL automated, robotic in situ method. Sections were scored in a blinded fashion to determine the extent of hepatocyte cell death. The surface area of the liver examined was equal in all instances and corresponded to 10 contiguous histologic fields at low magnification (×100).

In vivo IFN-γ and TNF-α infusion and β-gal staining

For in vivo studies, IFN-γ (5×10^4 U) or TNF-α (1×10^6 U) were administrated either alone or in combination through the portal vein of $fgl2^{-/-}$ and $fgl2^{+/+}$ mice. Liver tissues were collected at either 8 or 20 h postinfusion. β-gal staining was performed on tissue frozen in OCT (Tissue-Tek; Sakura Finetek) and sectioned on a cryostat at 6 μm. The β-gal staining kit (Invitrogen Life Technologies) was used and the protocol was modified for use on tissue sections to detect the Lac Z reporter. $fgl2^{-/-}$ and $fgl2^{+/+}$ mouse tissue samples were fixed in formaldehyde-glutaraldehyde and stained in a solution containing X-gal (40 mg/ml) in *N,N*-dimethylformamide for 24 h at 37°C in a humidified chamber. Each section was washed in PBS and covered with a coverslip in an aqueous mounting medium (DakoCytomation). $fgl2^{+/+}$ tissue was used as Lac Z-negative control. Serial sections were stained with H&E using standard procedures to confirm morphological structures seen by β-gal staining. For double staining, frozen sections were thawed at room temperature for 20 min. Slides were then fixed in 50% acetone and 50% methanol for 10 min. Slides were washed once in PBS containing 0.65% BSA, blocked for 30 min in wash buffer plus 3% goat serum and were analyzed using either the combination of rabbit anti-β-gal (Abcam) and rat anti-mouse CD31 (BD Biosciences) or rabbit anti-β gal and rat-anti-mouse CD11b (BD Biosciences). Second Abs were FITC-labeled goat-anti-rabbit IgG (Abcam) or rhodamine-labeled goat-anti-rat IgG (BD Biosciences).

Northern blot

Total cellular RNA (20 μg) from each tissue or cells was electrophoresed in a 1% denaturing agarose gel with 1.7% formaldehyde and then transferred to nitrocellulose membranes (Schleicher & Schuell) in 20× SSC (1× SSC in 0.15 M/L NaCl plus 0.015 M/L sodium citrate). RNA was immobilized by UV cross-linking the membrane, and hybridized in expresshyb from BD Clontech. Hybridization was conducted at 68°C for 2 h with an [α-^{32}P]dCTP-labeled 700-bp DNA probe of mouse fgl2 cDNA (7×10^8 cpm/μg) encompassing nt 100–639. Labeled mouse glyceraldehyde-3-phosphate dehydrogenase cDNA was used to ensure the equal loading of the RNA in each tissue. The membrane was washed twice with 1× SSC and 0.1% SDS at room temperature for 15 min and twice with 0.1× SSC and 0.5% SDS. The membrane was then autoradiographed by exposure to Kodak film (X-OMAT; Eastman Kodak).

fgl2 promoter constructs

fgl2 promoter reporter plasmids were constructed as described previously (20). Briefly, a 1.3-kb fgl2 promoter fragment was released from pM166 by digestion with *Sal*I and *Eco*RV and subcloned into pGL2Basic using the *Sma*I and *Xho*I sites in this vector to construct a promoter reporter plasmid pfgl2(−1320/+9)Luc. 5′ truncations of the fgl2 promoter in pGL2Basic were created by PCR. 5′-deleted promoter fragments were amplified from pfgl2(−1320/+9)Luc using a common antisense primer (5′-GCC ACA ACC AAC CAG GAA G-3′, positions 1335–1353 in GenBank accession AF025817) and a series of sense primers at varying distances upstream (20). The PCR products were subcloned into the plasmid PCR2.1 (Invitrogen Life Technologies). These fragments were then excised from PCR2.1 by digestion with *Hin*dIII and *Sal*I and transferred into the pGL2Basic using the *Hin*dIII and *Xho*I sites. All promoter constructs were sequenced to confirm the orientation and to verify the sequences.

Site-directed mutagenesis

Six sequential site-directed mutants were created within a 70-bp region (−119 to −41) of the fgl2 promoter in the promoter-reporter pfgl2(−1320/+9)Luc as described previously (20). Each mutant contains the sequence GGTACC, a *Kpn*I restriction site. These mutations were introduced using paired primers according to the manufacturer's instruction (Invitrogen Life Technologies). Mutants were verified by sequencing. Mutation of positions −108 to −99 and −97–91 (mut1 and 2) contains no known *cis* elements Mutation of positions −87 to −80 bp (mut3) contains an octamer motif: 5′-ATGCAAAT-3′. Mutation at positions −77 to −71 bp (mut4) contains a Sp1/Sp3-binding site 5′-GCCCGCCC-3′. Mutation at positions −68 to −59 bp contains the GAS/ETS binding site 5′-TTCTGGGAACT-3′. Mutation of positions −57 to −44 (mut6) contains an Ap1 site 5′-TGAGTCAG-3′.

Transient transfection and luciferase assay

Transient transfection was conducted using GenePorter (Gene Therapy System) according to manufacturer's instruction. RAW cells were plated at 5×10^5/well in 6-well plates 18 h before transfection. Transfection conditions were optimized using the SV40 promoter/enhancer luciferase control plasmid, pGL2-control. Cells were cotransfected with 2 μg of fgl2 reporter construct and 2 μg of pRSV-β-gal DNA to control for transfection efficiency as previously described (20). Each transfection experiment was performed in triplicate and repeated a minimum of three times.

EMSAs

Nuclear extracts from macrophage RAW cells were prepared as described (20). For EMSA, double-stranded GAS oligonucleotide probe (5′-GCC CTT TTC TGG GAA CTC AGA-3′, nt −76 to −56) was 5′ end-labeled with [γ-^{32}P]ATP (Amersham) using T4 polynucleotide kinase. fgl2 mutant 5′-CGCCCTTTTGAGGTACCTCAGAACGCCTG-3′ was used as competitor. The underlining represents the nucleotide changed. For each EMSA reaction, 2–5 μg of nuclear extracts were incubated for 15 min on ice in 20 μl of binding buffer. A total of 10^4 dpm of probe was added to each reaction and the mixture was incubated at room temperature for 30 min. For supershift assays, 2 μg of Ab were incubated with nuclear extracts for 45 min before adding DNA probe. Anti-STAT-1-α, Sp1, Sp3, ETS-1, PU.1 Elf-1, STAT-3 IgG are from Santa Cruz Biotechnology. For competition, 100× cold oligo was added to the reaction. The binding reactions were sized-fractionated on a nondenaturing, 5% acrylamide gel, and run at 150 V at room temperature for 2 h in 1 × Tris-glycine buffer.

Western blot

Cell lysates from a 10-cm plate were prepared by adding 0.5 ml of ice-cold buffer (20 mM Tris (pH 7.5), 150 mM NaCl, 1 mM EDTA, 1 mM EGTA, 1% Triton X-100, 2.5 mM sodium pyrophosphate) supplemented with the protease inhibitors leupeptin (1 μg/ml), pepstatin A (1 μg/ml), antipapin (50 μg/ml), and PMSF (0.1 mM). Lysates were scraped from the plate and sheared by passing through a 21-gauge needle three times. The lysates were centrifuged for 10 min at 4°C and the supernatants were collected. Samples were heated at 100°C for 5 min, cooled on ice, and resolved by SDS-PAGE, transferred to nitrocellulose membrane and subject to Ab detection. Anti-STAT-1, tyrosine phosphorylated STAT-1, p38, Lyn, tyrosine-phosphorylated p38, and serine 727-phosphorylated STAT-1 were obtained from Santa Cruz Biotechnology.

Chromatin immunoprecipitation assay (ChIP)

ChIP was performed on postconfluent cells using the ChIP Assay kit (Upstate Biotechnology) as previously described (21). Approximately 3×10^6 cells were used per ChIP assay. Briefly, formaldehyde was added to culture medium to a final concentration of 1%, and incubated for 10 min at 37°C following stimulation. Sonication of cell lysates achieved soluble chromatin fragments containing DNA ranging in size from 200 to 1000 bp. Sonicated cell lysates were centrifuged for 10 min at 14,000 rpm at 4°C. The supernatant was diluted 10 times to 2000 μl with ChIP dilution buffer. A 20-μl aliquot (1% of total) was removed, the cross-links were reversed by heating at 65°C for 4 h, and then 4 μl was used to quantitate the amount of input DNA. The remaining diluted supernatant was precleared with salmon sperm DNA/protein A agarose, then incubated overnight at 4°C with 5 μg of specific Ab (Ab), 5 μg of control rabbit IgG, or no Ab. To collect the immunoprecipitated (IP) complexes, salmon sperm DNA/protein A agarose was added and incubated for 1 h at 4°C. After washing, the immune complexes were eluted twice with 250 μl of freshly prepared elution buffer (1% SDS and 0.1 M NaHCO3). The formaldehyde cross-links were reversed in combined eluates by heating at 65°C for 4 h. The resulting IP DNA sample was purified and resuspended in 25 μl of filtered water. Twenty micrograms of tRNA was used to aid in precipitation. At least three independent ChIP assays were performed. Abs used for ChIP analysis were as follows: STAT1, PU.1, NF-κB, and RNA polymerase II (Pol II), purchased from Santa Cruz Biotechnology.

Real-time PCR analysis of ChIP samples

The following primer sets were used in ChIP experiments to amplify IP DNA containing the fgl2 promoter: for STAT1, PU.1 and Pol II of the fgl2 proximal promoter (−116 to −25), 5′-TCC TGT GTG GCG TCT GAG ACT-3′ and 5′-CTT TAA TAG CCA CCG CCG-3′; for NF-κB of the fgl2 upstream promoter region (−802 to −655), 5′-GAA TTT GGG TTT ATC TGT GTC AGT TAC GC-3′ and 5′-GGC TGT CCT TCC CCA TCA CTC AG-3′. The amount of target IP DNA was quantified on an ABI7900 HT sequence Detection System (Applied Biosystem) using SYBR green methodology. Determinations were performed in triplicate on 4 μl of bound chromatin, 4 μl of a no Ab control or control IgG immunoprecipitation, and 4 μl of a 10-fold diluted input chromatin in a 25-μl reaction. IP DNA was normalized to the diluted input sample using a $2^{-\Delta CT}$ calculation method (where CT is the cycle threshold) (22) and subtracts the no Ab or control IgG sample for nonspecific immunoprecipitation. Findings were comparable whether a no Ab control or control IgG was used to control for nonspecific immunoprecipitation.

Small-interfering RNA (siRNA)-based experiments

A siRNA strategy was used to examine the effects of silencing endogenous PU.1 on transcription of fgl2 in RAW cells. PU.1 and control siRNAs were obtained from Santa Cruz Biotechnology. Forty-eight hours after transfection with GeneSilencer (see below), total RNA or protein samples were prepared using the Qiagen total RNA kit or lysis buffer (see previous section). RT-PCR was performed to determine PU.1 expression at the mRNA level using the forward primer: CACCATGGAAGGGTTTTCCCT CACGTGG and reverse primer AGCCTGGCGGTCTCTGC.

For Western blotting, protein extracts from the same number of cells were loaded and were separated on a 10% SDS-PAGE gel and the proteins were detected with anti-PU.1 (Santa Cruz Biotechnology).

Cotransfection of siRNA and luciferase reporter plasmids was conducted using GeneSilencer siRNA Transfection Reagent (Gene Therapy System). For each transfection, 2 μg of luciferase reporter plasmid, 1 μg of pRSV-β-gal DNA, and 1 μg of siRNA were mixed based on GeneSilencer transfection manuals.

Data analysis

Data were expressed as mean ± SEM where applicable, obtained from at least three independent experiments, each done in triplicate. The Student *t* test for unpaired samples (two-tailed) was used to analyze the data. The level of statistically significant difference was defined as $p < 0.05$.

Results

IFN-γ and TNF-α induces fgl2 expression and causes hepatocyte apoptosis

As seen in Fig. 1, portal vein infusion of IFN-γ in combination with TNF-α led to apoptosis in >50% of hepatocytes (TUNEL staining). That hepatocyte apoptosis was fgl2 dependent was shown by the fact that liver tissue recovered from $fgl2^{-/-}$ mice infused with TNF-α and IFN-γ were near normal (Fig. 1). Intravascular fibrin deposits were seen adjacent to areas of hepatic necrosis and apoptosis, similar to mice infected with MHV-3 (17, 23). Infusion of IFN-γ or TNF-α alone failed to produce hepatocyte apoptosis (data not shown), suggesting that the combination of both cytokines is required for the induction of liver damage

β-gal staining was performed on liver tissue for detection of fgl2 promoter activity. Livers from wild-type control mice ($fgl2^{+/+}$) had no expression of fgl2 promoter-directed *Lac Z* gene, whereas patches of β-gal were seen in $fgl2^{-/-}$ mice 8 h after injection of IFN-γ as expected. Increased expression of β-gal persisted up to 20 h after IFN-γ injection (Fig. 2), with localization mainly near or along the vessels. Following infusion of TNF-α in $fgl2^{-/-}$ mice, β-gal activity was detected with a perivascular staining pattern within endothelial cells. Infusion of both TNF-α and IFN-γ resulted in enhanced β-gal staining in both macrophages and endothelial cells (Fig. 2). Macrophages and endothelial cells were confirmed as the cellular source of β-gal activity by immunofluorescence staining using anti-*CD11b* for macrophages and anti-CD31 for endothelial cells, as shown in Fig. 2.

Mechanism of IFN-γ-induced fgl2 transcription

As shown in Fig. 3, *IFN-γ*, but not TNF-α, IFN-α, IL-1, or LPS induced a time-dependent increase in fgl2 expression in RAW264.7 macrophage cells. RAW cells were transfected with the fgl2 promoter construct pfgl2(−1320/+9)Luc (20) to dissect the mechanism of IFN-γ-induced fgl2 expression. This construct has a 1320-bp DNA sequence upstream of the transcription start site. As shown in Fig. 4*A*, consistent with our Northern blot results (Fig. 3), IFN-γ induced fgl2 promoter activity to a maximum 8.5-fold, whereas IL-1 and TNF-α had no effect on fgl2 transcription. To identify functionally important DNA regions necessary for IFN-γ-induced fgl2 transcription, a series of plasmids containing a luciferase reporter under the control of successively deleted fgl2 promoters (20) were used. As shown in Fig. 4*B*, serial 5′-deletions of regions spanning −1.3 kb to −119 bp failed to eliminate fgl2 promoter activity in response to IFN-γ. Deletion of the region from −119 bp to −58 bp completely eliminated fgl2 promoter activity. This promoter region has previously been shown to be requisite for constitutive expression of fgl2 in endothelial cells and contains a cluster of *cis*-DNA elements including Oct-1, Sp1/Sp3, and an overlapping ETS/GAS or STAT-x site (20). One of these *cis* elements, the STATx/ETS-binding site (TTCTGGGAACT), or a GAS/ETS-like *cis* element, has been previously reported to bind to STAT proteins in response to IFNs (10). To test whether this *cis* element was responsible for fgl2 induction by IFN-γ, we mutated TTC TGG GAA CT to TTA TGG TAA CT in the pfgl2(−1320/+9)Luc and transfected this plasmid into RAW cells. Fig. 4*C* shows that this two-nucleotide mutation completely abrogated fgl2 promoter activity. In contrast, a mutation targeting an upstream IE1 *cis* element had no effect on fgl2 promoter activity. These

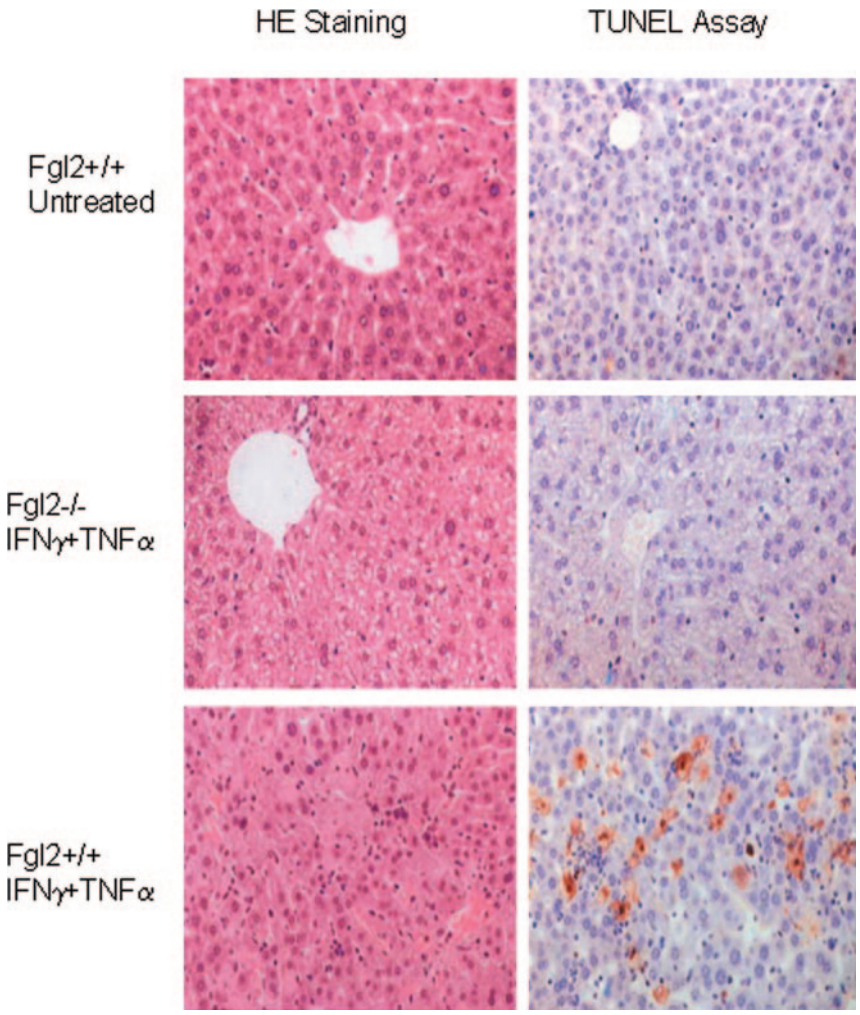

FIGURE 1. Histopathology of liver in $fgl2^{+/+}$ and $fgl2^{-/-}$ mice. Comparison of controls and mice following IFN-γ and/or TNF-α treatment. H&E-stained sections, *left panel*, the liver histology of either nontreated or combined IFN-γ and TNF-α-treated animals. *Right panel*, The TUNEL assay (by in situ hybridization) of the sequential sections to the *left*. All micrographs ×100 (original magnification).

results suggested that IFN-γ-induced fgl2 expression is dependent on STAT-x/ETS.

EMSAs were performed to examine the nature of the functionally important nucleoprotein complexes that form at STAT-x/ETS *cis*-regulating element important for IFN-γ induced fgl2 promoter activity in RAW cells. Using EMSA probe spanning nt −76/−57 containing the nucleotide sequence 5′-GCCCTT**TTCTGG GAACT**CAG-3′, we detected a specific protein-DNA complex following IFN-γ stimulation (Fig. 4*D*). (Bold and underlined portions of the sequence represent the STAT1 binding site.) Results showed that in resting cells, a single DNA-protein complex was observed (*lane 2*). After IFN-γ stimulation, an upper complex appeared on the gel (Fig. 4*D*, *lane 3*). The upper complex was specific because this complex could be competed away by 100-fold excess of cold probe (Fig. 4*D*, *lane 4*). Interestingly, a cold probe, 5′-GCCCTT**TTATGGTAACT**CAG-3′, which had the same mutation as the fgl2 promoter in Fig. 4*C*, only competed away the lower complex but not the upper complex (the one induced by IFN-γ treatment). At present, the lower band has not been identified and may represent nonspecific binding. In a supershift assay, an anti-STAT1 Ab was able to shift the upper complex (Fig. 4*D*, *lane 6*), whereas an anti-STAT3 Ab had no effect on the protein-DNA complexes (Fig. 4*D*, *lane 7*). To further assess the involvement of STAT1 in the transcription of fgl2 upon IFN-γ treatment, we examined whether STAT1 could bind to the GAS/ETS in the fgl2 proximal promoter in vivo. Binding of STAT1 was shown by the ChIP assay which showed a 27-fold increase of STAT1 with the fgl2 proximal promoter whereas the binding of Pol II to fgl2 increased 15-fold (Fig. 4*E*). These results collectively demonstrate that the macrophage GAS/ETS site was functional and active upon IFN-γ treatment, and that fgl2 induction by IFN-γ is STAT1 dependent.

IFN-γ-induced transcription of macrophage fgl2 depends on STAT-1/PU.1 cis *element and requires Sp1/Sp3-binding site*

As the region spanning from −119 to −59 bp of fgl2 promoter also includes OCT-1, Sp1/Sp3, as well Ap1 *cis*-DNA elements (Fig. 5), *cis* elements other than GAS/ETS were examined for their role in IFN-γ-induced fgl2 transcription. Reporter constructs containing six sequential mutated *cis* elements were transfected into RAW macrophage cells which were then stimulated with IFN-γ. As seen in Fig. 5*A*, while mut1, mut2, mut3 (mOct-1), and mut6 (mAP1) have no effect on IFN-γ-induced fgl2 transcription, mut4, which contains mutation of Sp1/Sp3 *cis* element, as well as mut5, which contains mutation of STAT1/ETS, significantly reduced fgl2 promoter activity. This result suggested that IFN-γ-induced fgl2 promoter activity also required the presence of an Sp1/Sp3-binding site. To confirm the involvement of an Sp1/Sp3 transcription factor in fgl2 promoter activity induced by IFN-γ, an adjacent probe to the STAT-1/ETS-containing Sp1/Sp3 site was examined for its binding ability to Sp1 or Sp3 in RAW cells. In contrast to that of endothelial cells (20), neither Sp1 nor Sp3 was able to bind to Sp1/Sp3 *cis* element without IFN-γ stimulation. The interaction with Sp1 and Sp3 was detected only when IFN-γ was added, as

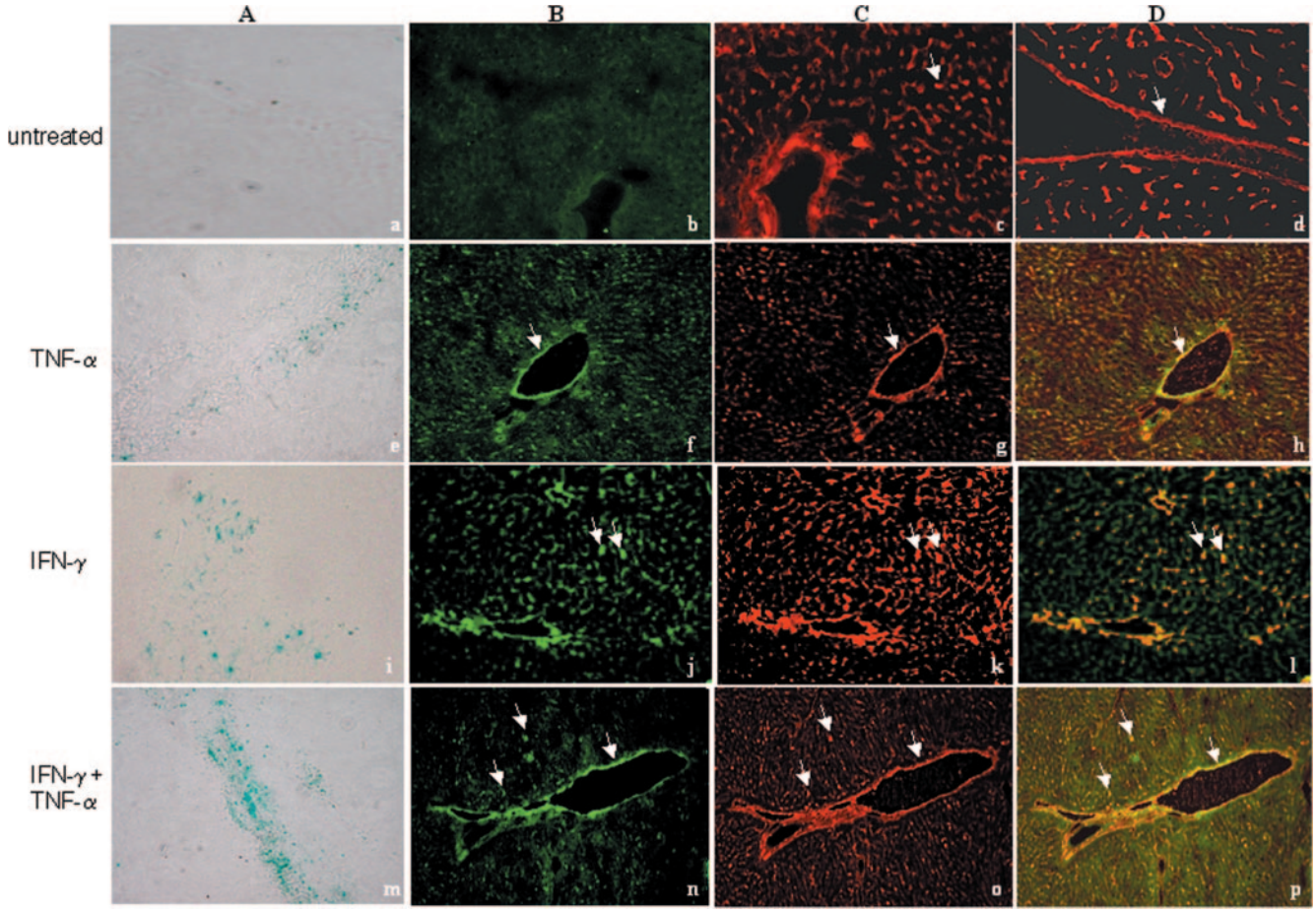

FIGURE 2. Cellular localization of fgl2 transcription in response to cytokine stimulation in hepatic tissue. Liver frozen sections were from *fgl2*$^{-/-}$ mice treated with TNF-α, IFN-γ, and combined TNF-α and IFN-γ and were stained as follows: *A*, β-Galactosidase (*a, e, i, and m*) using lacZ reporter blue. *B–D*, Immunofluorescence microscopy as follows: *B*, X-galactosidase FITC-labeled Ab (*b*, *f*, *j*, and *n*) green fluorescence. *C*, CD31 (*g*), *CD11b* (*c* and *k*), combined CD31 and CD11 (*o*), rhodamine-labeled Abs red fluorescence. *D*, *d*, CD31; *h*, *i*, and *p*, overlay of *B* and *C*; colocalization as shown by orange staining (arrows).

demonstrated by the supershift band seen following addition of either anti-Sp1 or anti-Sp3 Abs and the disappearance of the lower protein-DNA complex (Fig. 5*B*). The supershift pattern is similar to that seen in endothelial cells except for the appearance of an unidentified nonspecific complex (20). Both Sp1 and Sp3 are components of the protein-DNA complex formed with the Sp1/Sp3-binding site (Fig. 5*B*) suggesting that both transcription factors contribute to fgl2 induction in macrophage cells.

The involvement of Sp1/Sp3 in fgl2 induction, however, did not independently explain macrophage-specific induction by IFN-γ. In endothelial cells, both Sp1 and Sp3 were active and were able to interact with fgl2 promoter even without addition of IFN-γ (17, 20). Therefore, we postulated that additional *cis* elements might be invoked. The ETS core site, GGAA, located in the middle of the GAS/ETS element was examined for its possible role in differentiating the fgl2 induction by IFN-γ. EMSA was performed using the same probe for STAT1 (−76/−57) with macrophage nuclear extracts. As shown in Fig. 5*C*, without addition of IFN-γ there is a major complex seen in the gel which represents a nonspecific DNA-protein complex as seen in Fig. 4*D*. However, a shifted protein-DNA complex appeared after the addition of Ab against the ETS family member PU.1, while Ab against other ETS family members did not produce any shift. These results suggest that the PU.1-DNA complex might have been obscured in the major complex and the mutation of ETS core sequence GG GAA CT to GG TAA CT did not abolish the binding of PU.1 to the ETS core GGAA. The PU.1-STAT-1/ETS interaction was, however, further enhanced after addition of IFN-γ along with the STAT1-DNA complex (Fig. 5*D*). The ChIP assay was performed to further confirm the binding of PU.1 to the fgl2 proximal promoter containing GAS/ETS *cis* element in vivo. The direct immunoprecipitation of chromatin complex by anti-PU.1 showed that the PU.1-fgl2 promoter DNA complex increased 14-fold after IFN-γ treatment (Fig. 5*E*). As a similar protein-DNA complex was not detected when SVE-10 endothelial cell nuclear extracts were used (20), the interaction between PU.1 and STAT-1/PU.1 site suggested a distinctive function of PU.1 responsible for the induction of fgl2 in macrophages by IFN-γ and the lack of this factor (PU.1) in endothelial cells may explain the inability of IFN-γ to induce endothelial fgl2 transcription.

To confirm the involvement of PU.1 in macrophage fgl2 induction by IFN-γ, siRNA was used to silence the endogenous PU.1 expression in RAW cells because its binding site in the fgl2 promoter overlaps with that of STAT1. PU.1-specific and scrambled siRNAs were obtained from Santa Cruz Biotechnology. As seen in Fig. 6*A*, transfection of PU.1 siRNA resulted in significant reduction of the *PU.1* gene at the mRNA level as assessed by RT-PCR. Transfection of a control siRNA, a nonspecific sequence, had no effect on PU.1 expression compared with the no siRNA transfection control. The same results were obtained at the protein level as

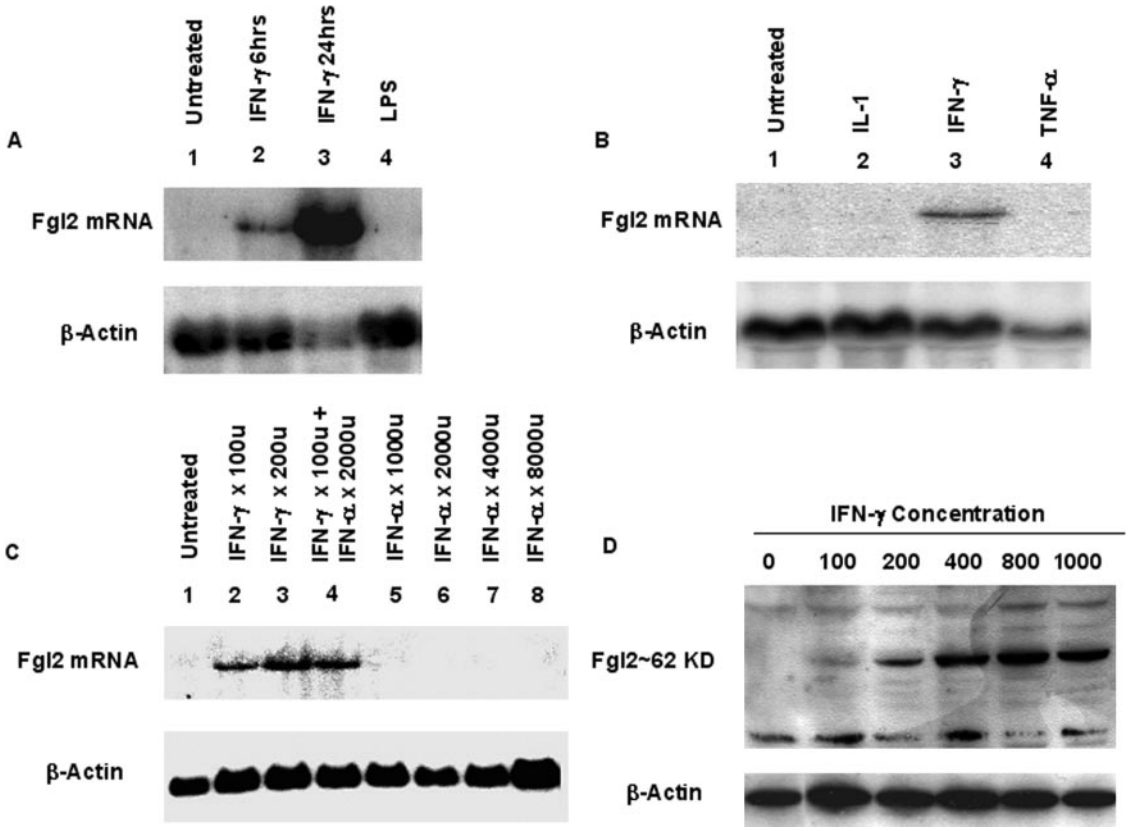

FIGURE 3. Cytokine induction of fgl2 mRNA and protein expression in macrophages. Northern blot analysis of fgl2 mRNA transcripts in macrophages. Twenty micrograms of total RNA extracted from unstimulated or cytokine stimulated RAW cells were added to each lane and hybridized with an fgl2 probe as described in *Materials and Methods.* An actin cDNA was used to ensure equal amounts of RNA in all lanes. *A*, RAW cells were incubated alone (untreated) for 24 h, *lane 1*; with 100 U/ml IFN-γ for 6 and 20 h, *lanes 2* and *3*; 50 ng/ml LPS, *lane 4*. *B*, RAW cells were incubated for 6 h alone (untreated), *lane 1*; or with 50 U/ml IL-1, *lane 2*; 100 U/ml IFN-γ, *lane 3*; and 400 U/ml TNF-α, *lane 4*. *C*, RAW cells untreated, *lane 1*; with 100 and 200 U/ml IFN-γ, *lanes 2* and *3*; 100 U/ml IFN-γ and 1000 U/ml IFN-α, *lane 4*, and increasing amount of IFN-α at 1000, 2000, 4000, and 8000 U/ml, *lanes 5–8. D*, fgl2 protein production in response to increasing concentrations of IFN-γ in peritoneal macrophages from BALB/cJ mice.

detected by Western blot with an anti-PU.1 Ab (Fig. 6*B*). As shown in Fig. 6*C*, cotransfection of a PU.1 siRNA with pfgl2LUC reporter plasmid significantly reduced fgl2 promoter activity in response to IFN-γ, while a control siRNA had no effect. These results argue for a role for PU.1 in macrophage fgl2 induction by IFN-γ.

Effect of IFN-γ and TNF-α on fgl2 transcription in macrophages and endothelial cells

On the basis of our in vivo studies, we postulated that TNF-α could enhance the fgl2 response to IFN-γ. As shown in Fig. 7*A*, IFN-γ induced macrophage fgl2 transcription, whereas TNF-α alone had no effect. When combined, however, TNF-α significantly enhanced IFN-γ induction of fgl2 expression in macrophages. In endothelial cells, the combination of TNF-α and IFN-γ led to more fgl2 mRNA expression than TNF-α alone. In both murine SVE-10 cells and in primary pig aorta endothelial cells, TNF-α alone induced fgl2 expression, whereas IFN-γ alone was ineffective (Fig. 7*B*). When both TNF-α and IFN-γ were added, fgl2 expression was enhanced (Fig. 7*C*). These studies show that IFN-γ and TNF-α can enhance each other's effect in fgl2 induction in different cells. However, the mechanism of TNF-α induction of fgl2 in endothelial cells and its enhancing effect by IFN-γ is still not clear and awaits further investigation

The mechanism of this enhancement in macrophages was examined further in vitro. RAW cells were transfected with the fgl2 promoter reporter constructs as described above. As shown in Fig. 7*D* the enhanced effect of TNF-α on IFN-γ transcription of fgl2 was localized between −725 and −614 bp upstream of the transcription start site (Fig. 7*D*). Within the negative strand three putative NF-κB-binding sites were identified. Addition of the NF-κB inhibitor MG132 abolished the enhanced TNF-α effect suggested the role of NF-κB in TNF-α-enhanced IFN-γ induction of fgl2 transcription (Fig. 7*E*). This result is further supported by a 4.7-fold increase in IP DNA by real-time PCR of the fgl2 promoter region containing putative NF-κB consensus-binding sites immunoprecipitated by anti-NF-κB Ab (Fig. 7*F*). Silencing of PU.1 using the same siRNA strategy described above also inhibited the ability of TNF-α to enhance IFN-γ-induced fgl2 transcription (Fig. 7*G*).

Discussion

In these studies, we document that portal vein infusion of IFN-γ in combination with TNF-α induces hepatocyte apoptosis that is dependent on expression of fgl2. This finding was confirmed by the observation that hepatocyte apoptosis was only seen in livers from $fgl2^{+/+}$ and not $fgl2^{-/-}$ mice. fgl2 mRNA and protein expression were induced by IFN-γ, but not by LPS, TNF-α, or IL-1 in isolated peritoneal macrophages or the RAW macrophage cell line. This macrophage-specific fgl2 induction by IFN-γ required a composite *cis* element that included Sp1/Sp3 and an overlapping GAS/ETS to interact with Sp1, Sp3, and STAT1. Furthermore, PU.1 regulated IFN-γ induction of fgl2 through the overlapping GAS/ETS site. Although TNF-α induced fgl2 transcription in endothelial cells, it

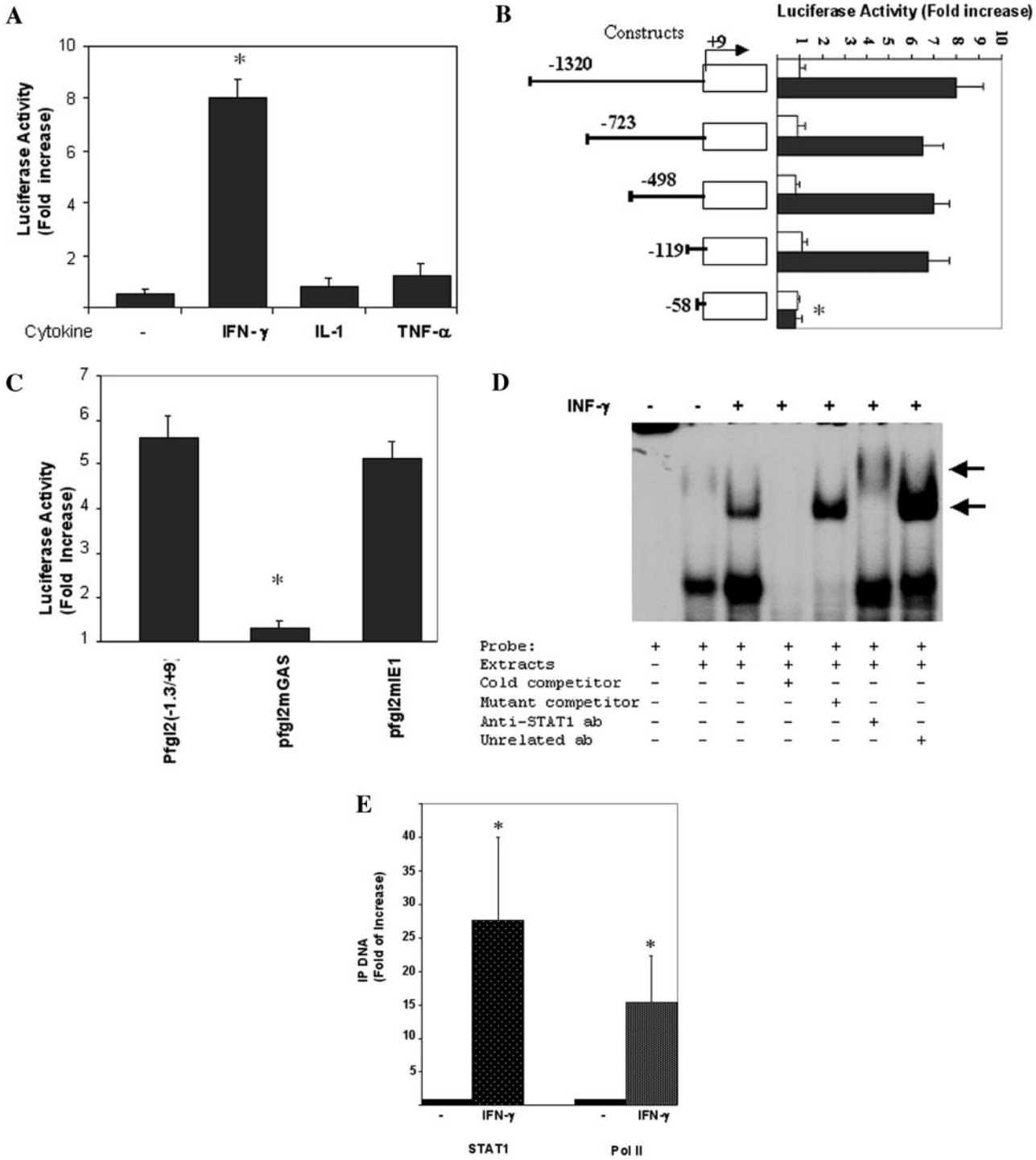

FIGURE 4. Identification of *cis*-DNA elements responsible for IFN-γ induction of fgl2. *A*, RAW cells were transfected with an fgl2 promoter reporter plasmid and unstimulated cells or cells stimulated with IFN-γ, IL-1, or TNF-α were analyzed for luciferase activity. ∗, A statistical difference between fgl2 promoter activities in IFN-γ-stimulated and untreated macrophages ($p < 0.05$). *B*, Analysis of fgl2 promoter activity with 5′-truncated fgl2 promoter reporter plasmids transfected into RAW cells and stimulated by IFN-γ. □, Untreated and ■, cells treated with IFN-γ. ∗, Promoter activity of pfgl2(−58/+9)Luc is significantly different from that of pfgl2(−1320/+9)Luc wild-type construct when macrophages were treated with IFN-γ. *C*, Contribution of putative GAS *cis* element to IFN-γ induction of fgl2. Putative GAS *cis* element and IE1 element were mutated in the fgl2 promoter reporter plasmid and transfected into RAW cells and analyzed for luciferase activity in response to IFN-γ treatment. ∗, Promoter activity of pfgl2mGASLuc is significantly different from that of pfgl2(−1320/+9)Luc wild-type construct in response to IFN-γ. From *A–C*, The data is the average of at least three separate experiments each performed in triplicate and are expressed as fold increase in luciferase activity ± SE relative to pfgl2(−1320/+9)Luc. The data was corrected for variation in transfection efficiency by normalization to the activity of a cotransfected plasmid expressing β-galactosidase. *D*, EMSA analysis of IFN-γ induced fgl2 transcription through the putative GAS element in the fgl2 promoter. Probe used is described in *Materials and Methods.* Nuclear extracts (NE) from RAW cells treated with or without IFN-γ were incubated with labeled probes. Addition of NE, cold probe competitors, and Abs are indicated at the *bottom* of the panel. Arrows indicate the specific STAT-1 DNA-protein complexes and Ab shifted DNA-protein complexes. *E*, ChIP assay was performed as described in *Materials and Methods.* fgl2 proximal promoter DNA pulled down was analyzed by real-time PCR. Data are expressed as fold increase in amount of DNA pulled down ± SD in IFN-γ-treated samples relative to that of no treatment. ∗, IP DNA from IFN-γ-treated cells by anti-STAT1 Ab is significantly different from that of untreated cells ($p < 0.05$).

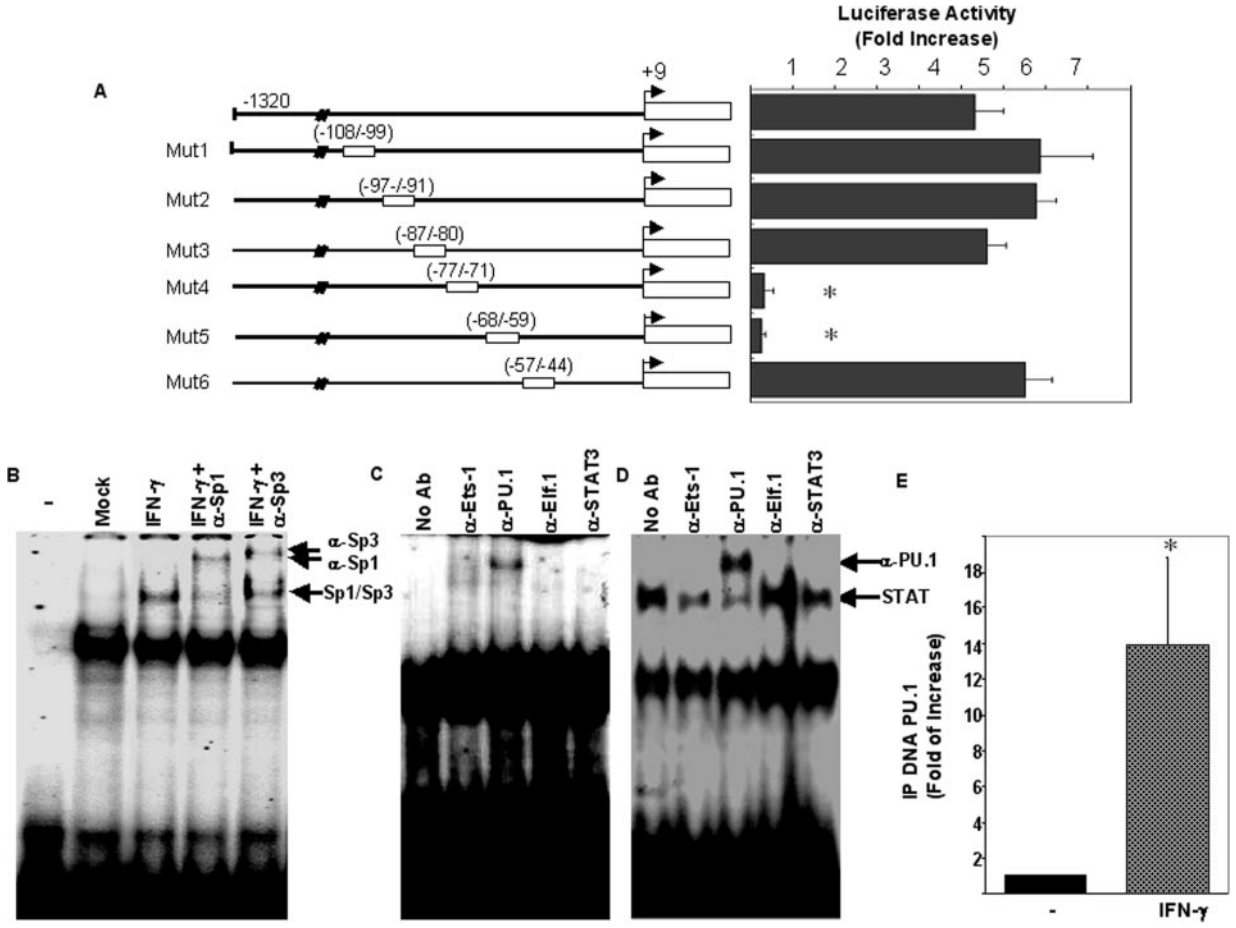

FIGURE 5. The involvement of *cis* elements in fgl2 transcription in response to IFN-γ. *A*, The effect of *cis* elements other than GAS/ETS on macrophage fgl2 transcription by IFN-γ was examined. Linker-scan mutants of fgl2 luciferase reporter plasmids were used as described in *Materials and Methods*. All mutant constructs were made using pfgl2(−1320/+9)Luc as template. The numbered boxes indicate the specific nucleotides mutated and their corresponding *cis* elements. Shown are representative experiments (triplicate determinations), each performed three times. Data are expressed as fold increase in luciferase activity ± SE relative to that of pfgl2(−1320/+9)Luc without IFN-γ treatment. ∗, Promoter activity of pfgl2mSp1/Sp3Luc (Mut4) and pfgl2mGAS/PU.1Luc (Mut5) was significantly different from that of wild-type construct pfgl2(−1320/+9)Luc in response to IFN-γ ($p < 0.05$). *B*, EMSA analysis of the protein-binding ability of Sp1/Sp3 and GAS/ETS *cis* element in macrophages. Arrows show the supershift complex with anti-Sp1 and anti-Sp3 Ab. *C* and *D*, Nuclear extracts from untreated and treated macrophages were incubated with labeled fgl2 probe −76/−57 fgl2 containing GAS/ETS *cis* element. Arrows show the supershift complex by anti-PU.1 Ab (*C* and *D*), and the appearance of STAT1 DNA-protein complex. *E*, ChIP assay of fgl2 proximal promoter DNA pulled down by real-time PCR. Shown are representative experiments (triplicate determinations), each performed at least three times. Data are expressed as fold increase in amount of DNA pulled down ± SD relative to that of no treatment. ∗, IP DNA from the IFN-γ-treated sample by anti-PU.1 Ab is significantly different from that of untreated sample ($p < 0.05$).

also enhanced IFN-γ-induced fgl2 transcription in macrophages. When IFN-γ and TNF-α were given together in vivo, both resident macrophages (Kupffer cells) and endothelial cells expressed fgl2 mRNA transcripts and protein, leading to fibrin deposition and hepatic apoptosis. Thus, our results suggest that the hepatocyte apoptosis requires the expression of both endothelial and macrophage fgl2. This finding is not totally unexpected as cytokine-induced spontaneous abortion is induced only by the combination of TNF-α and IFN-γ and not by either cytokine alone (24) Furthermore, TNF-induced hepatotoxicity only is seen when administered in combination with the hepatocyte-specific transcriptional inhibitor D-galactosamine (25). In the cytokine-induced fetal loss model, it was shown that copresence of endotoxin (LPS) and TNF-α and IFN-γ act synergistically. Thus, the data presented here in combination with previous studies supports the concept for the need for multiple simultaneous signals at the cellular level to trigger injury.

There is good evidence that IFN-γ plays an important role in liver damage. Hepatitis induced by administration of Con A is dependent on the expression of IFN-γ, and IFN-$\gamma^{-/-}$ mice show reduced liver damage (3). IFN-γ-dependent liver damage induced by Con A is via the Jak/STAT1 pathway. In this study, we show that IFN-γ induction of macrophage fgl2 is similarly induced through the Jak/STAT1 pathway. In the IFN-γ transgenic mouse model, the overexpression of IFN-γ results in pathologic findings of chronic active hepatitis, similar to human hepatitis (5). Additionally, IFN-γ has been found essential for hepatitis B virus surface Ag-specific cytotoxic T cell-mediated acute hepatitis (26).

The finding that IFN-γ induction of fgl2 expression is STAT1 dependent did not explain why IFN-γ could not induce fgl2 expression in other cell types. Although IFN-γ cannot induce fgl2 expression in endothelial cells, it is known that IFN-γ can activate the STAT1-signaling pathway in endothelial cells (27). This anomaly could be explained by our finding that PU.1, a B cell- and macrophage-specific ETS family member was required for fgl2 expression in macrophages and PU.1 is absent in endothelial cells.

PU.1 has been implicated in IFN-γ induction of CD40, FcR, and IL-18 expression in macrophages via constitutive binding to the

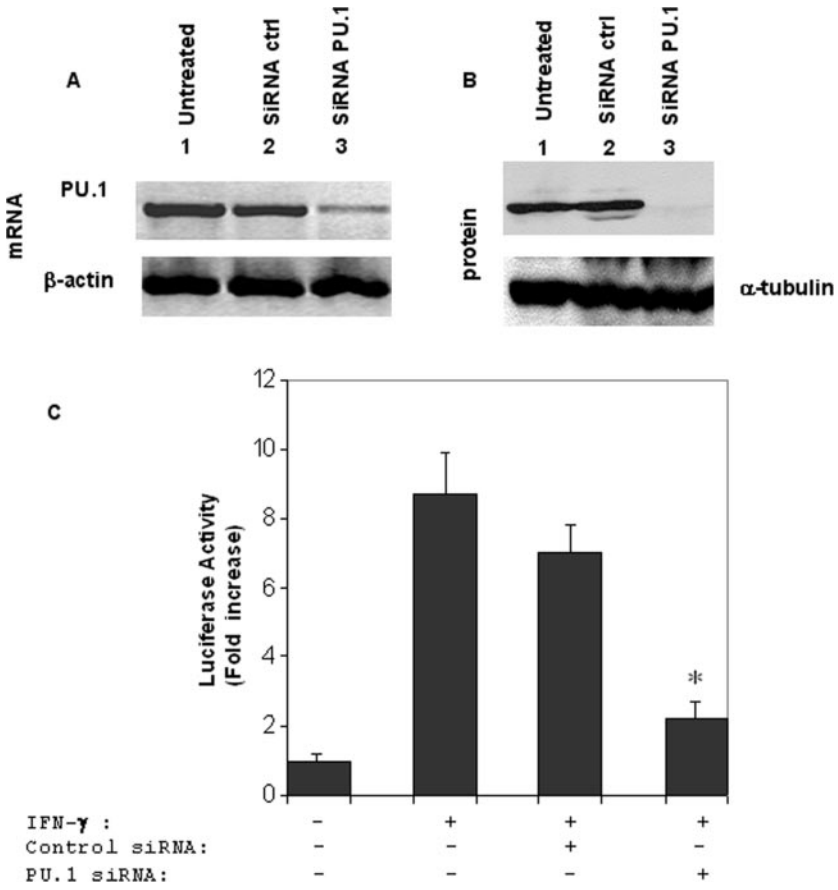

FIGURE 6. Effect of a PU.1 siRNA on fgl2 transcription. *A*, Transfection of RAW cells with PU.1 siRNA resulted in silencing of PU.1 gene transcription as assessed by RT-PCR. *Lane 1*, RAW cells, no treatment; *lane 2*, RAW cells treated with control siRNA; *lane 3*, RAW cells transfected with PU.1 siRNA. *B*, Effect of PU.1 siRNA transfection of RAW cells on PU.1 protein expression by Western blot. *Lane 1*, No treatment; *lane 2*, RAW cells transfected with control siRNA; *lane 3*, RAW cells transfected with PU.1 siRNA. *C*, RAW cells were cotransfected with an fgl2 promoter reporter construct and either control siRNA or PU.1 siRNA. IFN-γ was added as indicated in the figure. Shown are representative experiments (triplicate determinations), each performed three times. Data are expressed as fold increase in luciferase activity ± SE relative to that of pfgl2 (−1320/+9)Luc without IFN-γ and siRNA. ∗, The promoter activity pfgl2(−1320/+9)Luc in macrophages treated with PU.1 siRNA is significantly different from samples without siRNA treatment in response to IFN-γ ($p < 0.05$).

ETS cis element in the promoters of these genes (28–30). Furthermore, PU.1 facilitates the action of activated STAT1 (28–30). Meraro et al. (31) has shown interaction of PU.1 with a variety of IFN-stimulated response elements (on the composite ETS/IRF response element) to regulate cell-specific gene expression. Most of these genes can be induced by either a type I IFN or by both type I and type II IFN. However, the *fgl2* gene is different in that it is only induced by the type II IFN, IFN-γ. Although not totally explained, this difference may be due to the unique ETS/STAT1 composite that can bind both PU.1 and STAT1. Upon stimulation with IFN-γ, but not IFN-α, it appears that PU.1 and STAT1 form an efficient heterocomplex that can drive fgl2-specific expression in macrophages. Unlike CD40, FcR, and IL-18, which have separate STAT1- and PU.1-binding sites, the ETS core GGAA to which PU.1 binds in the fgl2 promoter is located in the middle of the overlapping GAS/ETS element, TTCTGGGAACT. (Underlined portion of the sequence represents the core binding site for Ets family of transcription factors.) In contrast to CD40, however, GAS and PU.1 had no spatial orientation and fgl2 also required the presence of the Sp1/Sp3-binding site or, specifically, the binding of the Sp1/Sp3 transcription factors. Thus, it is conceivable that the binding of Sp1/Sp3 in the presence of IFN-γ may serve as a core factor that recruits PU.1 to the adjacent GAS/ETS site. When cells were activated by IFN-γ, activated STAT1-α may have been able to recognize the GAS sequence and interact with both Sp1/Sp3 and PU.1 to drive the fgl2 transcription. A similar PU.1 protein-DNA complex was not detected in SVE-10 endothelial cells (20), and thus the lack of PU.1 may explain the inability of endothelial cells to express fgl2 in response to IFN-γ. Collectively, our studies demonstrate that while IFN-γ-induced fgl2 transcription is STAT1 dependent, binding of Sp1/Sp3 and PU.1 are necessary to ensure induction of fgl2 in macrophages.

There is now compelling evidence that suggests that local production of cytokines such as TNF-α and IFN-γ in T cell-driven models of fulminant hepatic failure are essential to the development of liver cell apoptosis (18). The local release of cytokines also exerts other effects, including interference with cell growth, leukocyte infiltration and activation, and up-regulation of vascular adhesion molecules (Ref. 32, ⟨www-ermm.cbcu.cam.ac.uk/01002812h.htm⟩). BALB/cJ mice following infection with MHV-3 develop fulminant hepatitis. In contrast to resistant A/J mice in which there is a transient and low-level production of IFN-γ and TNF-α, the expression of IFN-γ and TNF-α is sustained in high levels in susceptible BALB/cJ mice (33). Furthermore, only susceptible mice express fgl2 in response to MHV-3 which results in intravascular fibrin deposition and hepatocyte death. Thus, the additive effect of IFN-γ and TNF-α on the activation of fgl2 expression may contribute significantly to MHV-3-induced fulminant hepatitis in susceptible mice. Although we did not directly examine the mechanism for the increased apoptosis, initial unpublished data suggests that fgl2-induced apoptosis is independent of caspase activation.

The enhanced effects of the combination of the IFN-γ and TNF-α has also been reported in fetal loss syndrome in pregnant mice (34), and in the induction of diabetes in mice (35). The enhancing effects of IFN-γ and TNF-α in causing fetal loss could have been attributed to both macrophage and endothelial cell production of fgl2. However, the fetal loss could also be explained by enhanced fgl2 expression by only one cell type in response to the two cytokines. A previous report by Suk et al. (36) has shown a cellular signaling mechanism wherein IFN-γ acted via IRF-1 to phosphorylate STAT1 which in turn up-regulated the receptor for TNF-α that allowed TNF-α to activate cellular caspases. In this model, the two cytokines had to be present simultaneously. In the

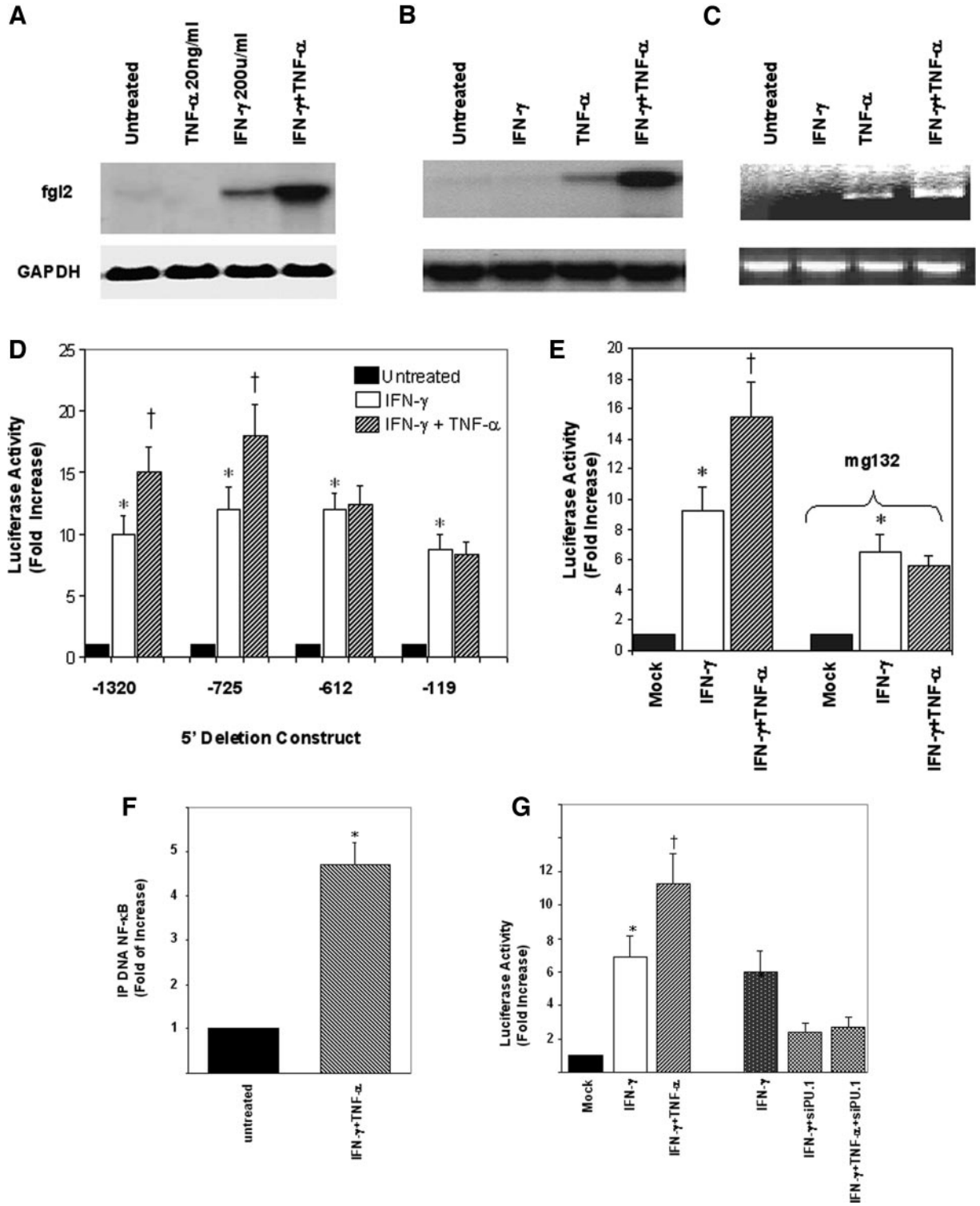

FIGURE 7. Synergistic effect of IFN-γ and TNF-α on macrophage fgl2 mRNA transcription. *A*, TNF-α enhances IFN-γ-induced fgl2 transcription in macrophages. *B* and *C*, IFN-γ enhanced TNF-α-induced fgl2 transcription in primary pig endothelial cells (*B*) and in the mouse endothelial cell line SVE-10 (*C*). *D*, Localization of *cis* elements responsible for TNF-α-enhanced fgl2 transcription in response to IFN-γ. A series of truncated fgl2 promoter reporter plasmids, including pfgl2(−1320/+9)Luc, pfgl2(−723/+9)Luc, pfgl2(−612/+9)Luc were transfected into macrophage cells. Transfected cells were either treated with either IFN-γ or IFN-γ plus TNF-α 24 h posttransfection. Numbers indicate the location of truncation upstream of fgl2 transcription start site. *E*, TNF-α enhanced IFN-γ induction of fgl2 transcription in macrophages was blocked by mg132, an NF-κB inhibitor. *F*, ChIP assay of fgl2 proximal promoter DNA pulled down by anti-NF-κB Ab by real-time PCR. ∗, IP DNA from an IFN-γ- and TNF-α-treated sample by NF-κB Ab is significantly different from that of untreated sample. *G*, siRNA against PU.1 inhibited both *IFN*-γ and the combination of *IFN*-γ and TNF-α induced fgl2 promoter activity. For all experiments, 20 ng/ml TNF-α and 200 U/ml IFN-γ were used through *A–F*. *D* and *G* are representative experiments (triplicate determinations), each performed at least three times. Data are expressed as fold increase in luciferase activity ± SE relative to that of pfgl2(−1320/+9)Luc without IFN-γ treatment or fold increase ± SD in DNA immunoprecipitated (pull-down assay) as analyzed by real-time PCR. ∗, The promoter activity following IFN-γ or TNF-α treatment is significantly different from that of the untreated samples ($p < 0.05$). †, The promoter activity after the addition of TNF-α in the presence of IFN-γ is significantly different from samples treated by IFN-γ alone ($p < 0.05$).

present study, enhancement was noted at the single-cell level in both macrophages and endothelial cells. The exact pathways whereby TNF-α enhances the effect of IFN-γ in macrophages (and vice versa in endothelial cells) have not been determined. It is probably distinct from those described by Suk et al. (36) and related to the interaction of NF-κB to the upstream fgl2 promoter region (Fig. 7*F*). Further studies are now ongoing to determine the exact DNA *cis* element requirement for this interaction. The existence of complex cell type-specific molecular cascades regulating fgl2 expression is consistent with fgl2 being a powerful biological mediator. This study demonstrated that IFN-γ and TNF-α play a critical role in fgl2-dependent hepatic cell death (apoptosis), suggesting that targeting of both IFN-γ and TNF-α-mediated transcriptional pathways in specific cell types may lead to the modulation of the fgl2 expression and help to prevent liver injury.

Disclosures

The authors have no financial conflict of interest.

References

1. Schattner, A. 1994. Lymphokines in autoimmunity–a critical review. *Clin. Immunol. Immunopathol.* 70: 177–189.
2. Winwood, P. J., and M. J. Arthur. 1993. Kupffer cells: their activation and role in animal models of liver injury and human liver disease. *Semin. Liver Dis.* 13: 50–59.
3. Hong, F., B. Jaruga, W. H. Kim, S. Radaeva, O. N. El Assal, Z. Tian, V. A. Nguyen, and B. Gao. 2002. Opposing roles of STAT1 and STAT3 in T cell-mediated hepatitis: regulation by SOCS. *J. Clin. Invest.* 110: 1503–1513.
4. Kim, W. H., F. Hong, S. Radaeva, B. Jaruga, S. Fan, and B. Gao. 2003. STAT1 plays an essential role in LPS/D-galactosamine-induced liver apoptosis and injury. *Am. J. Physiol.* 285: G761–G768.
5. Toyonaga, T., O. Hino, S. Sugai, S. Wakasugi, K. Abe, M. Shichiri, and K. Yamamura. 1994. Chronic active hepatitis in transgenic mice expressing interferon-γ in the liver. *Proc. Natl. Acad. Sci. USA* 91: 614–618.
6. Ando, K., T. Moriyama, L. G. Guidotti, S. Wirth, R. D. Schreiber, H. J. Schlicht, S. N. Huang, and F. V. Chisari. 1993. Mechanisms of class I restricted immunopathology: a transgenic mouse model of fulminant hepatitis. *J. Exp. Med.* 178: 1541–1554.
7. Briscoe, J., N. C. Rogers, B. A. Witthuhn, D. Watling, A. G. Harpur, A. F. Wilks, G. R. Stark, J. N. Ihle, and I. M. Kerr. 1996. Kinase-negative mutants of JAK1 can sustain interferon-γ-inducible gene expression but not an antiviral state. *EMBO J.* 15: 799–809.
8. Heim, M. H., I. M. Kerr, G. R. Stark, and J. E. Darnell, Jr. 1995. Contribution of STAT SH2 groups to specific interferon signaling by the Jak-STAT pathway. *Science* 267: 1347–1349.
9. Greenlund, A. C., M. O. Morales, B. L. Viviano, H. Yan, J. Krolewski, and R. D. Schreiber. 1995. Stat recruitment by tyrosine-phosphorylated cytokine receptors: an ordered reversible affinity-driven process. *Immunity* 2: 677–687.
10. Look, D. C., M. R. Pelletier, and M. J. Holtzman. 1994. Selective interaction of a subset of interferon-γ response element-binding proteins with the intercellular adhesion molecule-1 (ICAM-1) gene promoter controls the pattern of expression on epithelial cells. *J. Biol. Chem.* 269: 8952–8958.
11. Chang, Y. J., M. J. Holtzman, and C. C. Chen. 2002. Interferon-γ-induced epithelial ICAM-1 expression and monocyte adhesion: involvement of protein kinase C-dependent c-Src tyrosine kinase activation pathway. *J. Biol. Chem.* 277: 7118–7126.
12. Roy, S. K., S. J. Wachira, X. Weihua, J. Hu, and D. V. Kalvakolanu. 2000. CCAAT/enhancer-binding protein-β regulates interferon-induced transcription through a novel element. *J. Biol. Chem.* 275: 12626–12632.
13. Ulgiati, D., L. S. Subrata, and L. J. Abraham. 2000. The role of Sp family members, basic Kruppel-like factor, and E box factors in the basal and IFN-γ regulated expression of the human complement C4 promoter. *J. Immunol.* 164: 300–307.
14. Ding, J. W., Q. Ning, M. F. Liu, A. Lai, J. Leibowitz, K. M. Peltekian, E. H. Cole, L. S. Fung, C. Holloway, P. A. Marsden, et al. 1997. Fulminant hepatic failure in murine hepatitis virus strain 3 infection: tissue-specific expression of a novel fgl2 prothrombinase. *J. Virol.* 71: 9223–9230.
15. Ning, Q., S. Lakatoo, M. Liu, W. Yang, Z. Wang, M. J. Phillips, and G. A. Levy. 2003. Induction of prothrombinase fgl2 by the nucleocapsid protein of virulent mouse hepatitis virus is dependent on host hepatic nuclear factor-4 α. *J. Biol. Chem.* 278: 15541–15549.
16. Li, C., L. S. Fung, S. Chung, A. Crow, N. Myers-Mason, M. J. Phillips, J. L. Leibowitz, E. Cole, C. A. Ottaway, and G. Levy. 1992. Monoclonal anti-prothrombinase (3D4.3) prevents mortality from murine hepatitis virus (MHV-3) infection. *J. Exp. Med.* 176: 689–697.
17. Marsden, P. A., Q. Ning, L. S. Fung, X. Luo, Y. Chen, M. Mendicino, A. Ghanekar, J. A. Scott, T. Miller, C. W. Chan, et al. 2003. The Fgl2/fibroleukin prothrombinase contributes to immunologically mediated thrombosis in experimental and human viral hepatitis. *J. Clin. Invest.* 112: 58–66.
18. Pope, M., O. Rotstein, E. Cole, S. Sinclair, R. Parr, B. Cruz, R. Fingerote, S. Chung, R. Gorczynski, L. Fung, et al. 1995. Pattern of disease after murine hepatitis virus strain 3 infection correlates with macrophage activation and not viral replication. *J. Virol.* 69: 5252–5260.
19. Lafuse, W. P., L. Castle, D. Brown, and B. S. Zwilling. 1995. The cytotoxic T lymphocyte gene FIBLP with homology to fibrinogen β and γ subunits is also induced in mouse macrophages by IFN-γ. *Cell. Immunol.* 163: 187–190.
20. Liu, M., J. L. Leibowitz, D. A. Clark, M. Mendicino, Q. Ning, J. W. Ding, C. D'Abreo, L. Fung, P. A. Marsden, and G. A. Levy. 2003. Gene transcription of fgl2 in endothelial cells is controlled by Ets-1 and Oct-1 and requires the presence of both Sp1 and Sp3. *Eur. J. Biochem.* 270: 2274–2286.
21. Chan, G. C., J. E. Fish, I. A. Mawji, D. D. Leung, A. C. Rachlis, and P. A. Marsden. 2005. Epigenetic basis for the transcriptional hyporesponsiveness of the human inducible nitric oxide synthase gene in vascular endothelial cells. *J. Immunol.* 175: 3846–3861.
22. Herman, A. E., G. J. Freeman, D. Mathis, and C. Benoist. 2004. $CD4^+CD25^+$ T regulatory cells dependent on ICOS promote regulation of effector cells in the prediabetic lesion. *J. Exp. Med.* 199: 1479–1489.
23. Levy, G. A., M. Liu, J. Ding, S. Yuwaraj, J. Leibowitz, P. A. Marsden, Q. Ning, A. Kovalinka, and M. J. Phillips. 2000. Molecular and functional analysis of the human prothrombinase gene (HFGL2) and its role in viral hepatitis. *Am. J. Pathol.* 156: 1217–1225.
24. Clark, D. A., J. Manuel, L. Lee, G. Chaouat, R. M. Gorczynski, and G. A. Levy. 2004. Ecology of danger-dependent cytokine-boosted spontaneous abortion in the CBA $\times$ DBA/2 mouse model. I. Synergistic effect of LPS and (TNF-α + IFN-γ) on pregnancy loss. *Am. J. Reprod. Immunol.* 52: 370–378.
25. Wullaert, A., B. Wielockx, S. Van Huffel, V. Bogaert, B. De Geest, P. Papeleu, P. Schotte, K. El Bakkouri, K. Heyninck, C. Libert, and R. Beyaert. 2005. Adenoviral gene transfer of ABIN-1 protects mice from TNF/galactosamine-induced acute liver failure and lethality. *Hepatology* 42: 381–389.
26. Guidotti, L. G., and F. V. Chisari. 1996. To kill or to cure: options in host defense against viral infection. *Curr. Opin. Immunol.* 8: 478–483.
27. Ruegg, C., A. Yilmaz, G. Bieler, J. Bamat, P. Chaubert, and F. J. Lejeune. 1998. Evidence for the involvement of endothelial cell integrin $\alpha_V\beta_3$ in the disruption of the tumor vasculature induced by TNF and IFN-γ. *Nat. Med.* 4: 408–414.
28. Nguyen, V. T., and E. N. Benveniste. 2000. Involvement of STAT-1 and ets family members in interferon-γ induction of CD40 transcription in microglia/macrophages. *J. Biol. Chem.* 275: 23674–23684.
29. Kim, Y. M., H. S. Kang, S. G. Paik, K. H. Pyun, K. L. Anderson, B. E. Torbett, and I. Choi. 1999. Roles of IFN consensus sequence binding protein and PU.1 in regulating IL-18 gene expression. *J. Immunol.* 163: 2000–2007.
30. Eichbaum, Q. G., R. Iyer, D. P. Raveh, C. Mathieu, and R. A. Ezekowitz. 1994. Restriction of interferon γ responsiveness and basal expression of the myeloid human FcγR1b gene is mediated by a functional PU.1 site and a transcription initiator consensus. *J. Exp. Med.* 179: 1985–1996.
31. Meraro, D., M. Gleit-Kielmanowicz, H. Hauser, and B. Z. Levi. 2002. IFN-stimulated gene 15 is synergistically activated through interactions between the myelocyte/lymphocyte-specific transcription factors, PU.1, IFN regulatory factor-8/IFN consensus sequence binding protein, and IFN regulatory factor-4: characterization of a new subtype of IFN-stimulated response element. *J. Immunol.* 168: 6224–6231.
32. Liu, M., C. W. Chan, I. D. McGilvray, Q. Ning, and G. A. Levy. 2001. Fulminant viral hepatitis: molecular and cellular basis, and clinical implications. *Exp. Rev. Mol. Med.* 3: 1-19.
33. Mello, I. G., R. C. Vassao, and C. A. Pereira. 1993. Virus specificity of the antiviral state induced by IFN-γ correlates with resistance to MHV 3 infection. *Arch. Virol.* 132: 281–289.
34. Clark, D. A., G. Chaouat, P. C. Arck, H. W. Mittruecker, and G. A. Levy. 1998. Cytokine-dependent abortion in CBA $\times$ DBA/2 mice is mediated by the procoagulant fgl2 prothrombinase (correction of prothrombinase). *J. Immunol.* 160: 545–549.
35. Suk, K., S. Kim, Y. H. Kim, K. A. Kim, I. Chang, H. Yagita, M. Shong, and M. S. Lee. 2001. IFN-γ/TNF-α synergism as the final effector in autoimmune diabetes: a key role for STAT1/IFN regulatory factor-1 pathway in pancreatic β cell death. *J. Immunol.* 166: 4481–4489.
36. Suk, K., I. Chang, Y. H. Kim, S. Kim, J. Y. Kim, H. Kim, and M. S. Lee. 2001. Interferon γ (IFN-γ) and tumor necrosis factor α synergism in ME-180 cervical cancer cell apoptosis and necrosis: IFN-γ inhibits cytoprotective NF-κB through STAT1/IRF-1 pathways. *J. Biol. Chem.* 276: 13153–13159.